



Development of Bearing Capacity Equation for Rectangular Footing under Inclined Loading on Layered Sand

Panwar, V.^{1*}  and Dutta, R.K.² 

¹ Ph.D. Candidate, Department of Civil Engineering, National Institute of Technology Hamirpur, Hamirpur, Himachal Pradesh, India.

² Professor, Department of Civil Engineering, National Institute of Technology Hamirpur, Hamirpur, Himachal Pradesh, India.

© University of Tehran 2022

Received: 21 Feb. 2022;

Revised: 15 May 2022;

Accepted: 15 Jun. 2022

ABSTRACT: This study provides an equation of bearing capacity for a rectangular footing placed on dense sand overlying loose sand and subjected to inclined concentric loading using the limit equilibrium followed by projected area method. The parameters varied were thickness ratio (0.00 to 2.00) of the upper dense sand layer, embedment ratio (0 to 2), friction angle of upper dense (41° to 46°) sand and lower loose (31° to 36°) sand layer, and applied load inclination (0° to 30°) for the parametric study. The highest and lowest increase in the bearing capacity were observed for a friction angle combination of 46° - 36° and 41° - 31° , respectively, at different thickness ratios. The bearing capacity obtained from the proposed equation was approximately 4.97 and 10.5 times its initial value at embedment ratios of 1 and 2, respectively. Bearing capacity was reduced by 20.55%, 54.58% and 87.90% for load inclinations of 5° , 15° , and 30° for friction angles of upper dense and lower loose sand layer combinations of 46° and 36° and at a thickness ratio of 2. The bearing capacity obtained from the proposed equation decreased by 99.89%, 66.04%, and 61.5% as the load inclination increased from 0° to 30° for embedment ratios of 0, 1, and 2. With respect to finite element results, the average deviation of the bearing capacity obtained from the proposed equation at embedment ratios 0, 1, and 2 was 14.56%, 18.71% and 23.56%, respectively. The proposed bearing capacity equation produced results that were consistent with those reported in the literature, with an average deviation of 10.71%.

Keywords: Bearing Capacity, Inclined Loading, Layered Sand, Projected Area Approach, Rectangular Footing.

1. Introduction

The load of the superstructure through the footing is shifted to the soil underneath it. The depth-to-width ratio determines whether a footing is shallow or deep. The load must be transferred underneath the

footing in a way that avoids settling and shear failure. In the literature, a number of studies have been reported by the researchers (Meyerhof, 1974; Meyerhof and Hanna, 1978; Hanna, 1981, 1982, 1987; Oda and Win, 1990; Michalowski and Shi, 1995; Kenny and Andrawes, 1997;

* Corresponding author E-mail: vipsarahan17@gmail.com

Okamura et al., 1998; Merifield et al., 1999; Shiau et al., 2003; Farah, 2004; Massih et al., 2005; Kumar et al., 2007; Johnson et al., 2015; Mosadegh and Nikraz, 2015; Rao et al., 2015; Ibrahim, 2016; Khatri et al., 2017a; Misir and Laman, 2017; Saha et al., 2018; Reddy and Kumar, 2018; Eshkevari et al., 2018; Eshkevari et al., 2019; Zheng et al., 2019; Biswas and Krishna, 2019; Ullah et al., 2020; Chwała and Puła, 2020; Al-Ameri et al., 2020; Benmoussa et al., 2021; Mandeel et al., 2021; Panwar and Dutta, 2021; Singh and Rao, 2021; Nujid et al., 2021; Ibrahim et al., 2021; Das and Khatri, 2021; Gupta and Mital, 2021; Hajitaheriha et al., 2021 and Das et al., 2022) to evaluate the bearing capacity of footings on single layer or layered soils and subjected to vertical or inclined loads.

Meyerhof (1974), Khatri et al. (2017a), Eshkevari et al. (2019) and Das and Khatri (2021) investigated the bearing capacity of strip and circular footing on layered soil (dense sand over loose sand) under vertical load. Further, Oda and Win (1990), Meyerhof (1974), Michalowski and Shi (1995), Okamura et al. (1998), Farah (2004), Kumar et al. (2007), Mosadegh and Nikraz (2015), Misir and Laman (2017), Reddy and Kumar (2018), Saha et al. (2018), Biswas and Krishna (2019), Al-Ameri et al. (2020), Chwała and Puła (2020) and Nujid et al. (2021) studied the bearing capacity of the strip, circular and square/rectangular footing on layered soil (dense sand over soft clay) under vertical load. The bearing capacity of the strip, circular and rectangular footing on layered soil (stiff clay over soft clay, stiff over soft clay and stiff clay over loose sand) was conducted by Rao et al. (2015), Ullah et al. (2020), Benmoussa et al. (2021) and Ibrahim et al. (2021) under vertical loading. In addition, there were studies (Meyerhof and Hanna, 1978; Hanna, 1981, 1982; Massih et al., 2005; Mosadegh and Nikraz, 2015) on bearing capacity for strip and circular footings on layered soil (dense sand over loose sand; loose sand over dense sand; and dense sand over soft clay)

available in the literature. Under vertical (Meyerhof, 1974; Kenny and Andrawes, 1997; Okamura et al., 1998) and inclined (Meyerhof and Hanna, 1978) loads, the limit equilibrium approach was employed to investigate the bearing capacity of the strip and circular footings.

Using the punching shear coefficient for the vertical and inclined loading, an equation for the ultimate bearing capacity of strip and circular footings on layered soil (dense sand over loose sand) was suggested by Meyerhof (1974) and Meyerhof and Hanna (1978). Comparison of the findings of Meyerhof (1974), Meyerhof and Hanna (1978) and Kenny and Andrawes (1997) was attempted by Shoaie et al. (2012) and concluded that the findings of Meyerhof (1974) and Meyerhof and Hanna (1978) overestimate the bearing capacity at greater depths. Michalowski and Shi (1995) used a Kinematic approach for estimation of average pressure below the strip footing under vertical loading. Projected area approach was followed by Kenny and Andrawes (1997), Okamura et al. (1998) and Farah (2004) to estimate the bearing capacity of the strip, circular and square/rectangular footing on layered soil under vertical loading.

In order to predict the ultimate bearing capacity for strip, circular and square/rectangular footing on layered soil (dense sand over soft clay) using punching shear coefficients, load dispersion angle and soil properties under vertical loading, an equation was proposed by Farah (2004) and it was found to overestimate the bearing capacity as compared to previous studies Meyerhof (1974). Further, the researchers Misir and Laman (2017) and Al-Ameri et al. (2020) developed the bearing capacity equation using regression analysis based on the limit equilibrium analysis and finite element analysis for circular and square footing. The results were in a very good agreement to predict the bearing capacity when compared with the past works. Recently Finite Element modelling was used to assess the bearing capacity of strip

(Hanna, 1987; Mosadegh and Nikraz, 2015; Khatri et al., 2017a; Eshkevariet al., 2018; Das and Khatri, 2021; Nujid et al., 2021), circular (Khatri et al., 2017a; Reddy and Kumar, 2018; Singh and Rao, 2021; Das and Khatri, 2021; Benmoussa et al., 2021), square (Saha et al., 2018; Mandeel et al., 2021) and rectangular (Ullah et al., 2020; Panwar and Dutta, 2021; Ibrahim et al., 2021) footings on layered soil (dense sand over loose sand, dense sand over soft clay, soft clay over dense sand and soft clay over stiff clay), respectively.

Gupta and Mital (2021) investigated the effect of multilayer of geogrid reinforced sand on the bearing capacity of rectangular footing under inclined as well as eccentric loading experimentally. The effect of various parameters such as number of reinforced layers, eccentricity and load inclination were investigated using laboratory tests and finite element analysis. The ultimate bearing capacity observed to be increased with the increase in geogrid reinforced layers. Das et al. (2022) investigated the effect of geogrid sheet reinforced at the interface of dense sand and loose sand for the ultimate bearing capacities of embedded strip and circular footing and concluded that the effect of geogrid sheet was marginal when compared with the ultimate bearing capacity of unreinforced foundation.

Using the Finite Element analysis, Hajitaheriha et al. (2021) examined the impact on drag stress of the circular and square section piles placed in soft clay overlaid on dense sand. In the circular sections, the value of the drag load was always greater when compared with the results for the square-shaped sections pile. The ultimate bearing capacity was calculated using numerical and experimental methods in all the above studies. However, no equation of ultimate bearing capacity for the rectangular footing under inclined loading has been published since then, especially on layered soil (dense sand over loose sand). As a result, using the punching shear mechanism and limit

equilibrium methodology, an equation for the bearing capacity of rectangular footing on dense sand underlain by loose sand under inclined loading was derived in the current study. To get a fair estimate of bearing capacity, the load spread mechanism in the upper dense sand layer was selected using finite element analysis. The bearing capacity of the rectangular footing over layered sand was calculated for various friction angles of upper dense and lower loose sand layer, load inclination and varied thickness of upper dense sand layer at different footing depths. The findings were compared to those found in the literature.

2. Methodology

Following the limit equilibrium approach reported by Meyerhof and Hanna (1978), the load from the footing was assumed to spread through the upper dense sand to the lower loose sand. The failure surface for rectangular footing under load (q_u) with load inclination (θ) is shown in Figure 1a. The footing is placed at a depth (D) below the surface of ground level and the passive pressure (P_p) was assumed to act on the failure surface by making angle δ normal to the failure surface. The failure was assumed to occur at the interface of the upper dense and lower loose sand layer. Figure 1b shows a plan view of the assumed failure mechanism under inclined loading (q_u) for the rectangular footing with load dispersion angle α_1 and α_2 across the width and α_3 and α_4 across the length of the footing. The assumptions made for mathematical derivation are as follows.

- The footing is assumed to have rigid and rough base lying at some depth (D) in upper dense sand layer.
- The sand above the footing base has negligible shear strength and it acts as a surcharge load.
- The interface of the layered sand and the ground surface is assumed to be horizontal.
- No effect of the water table on the

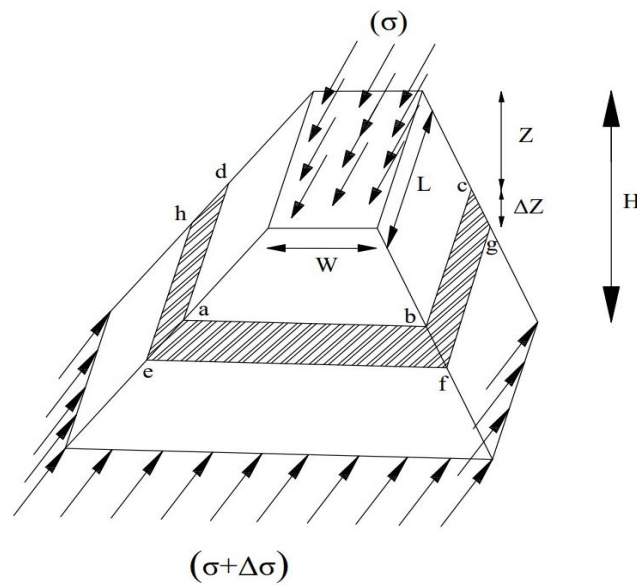


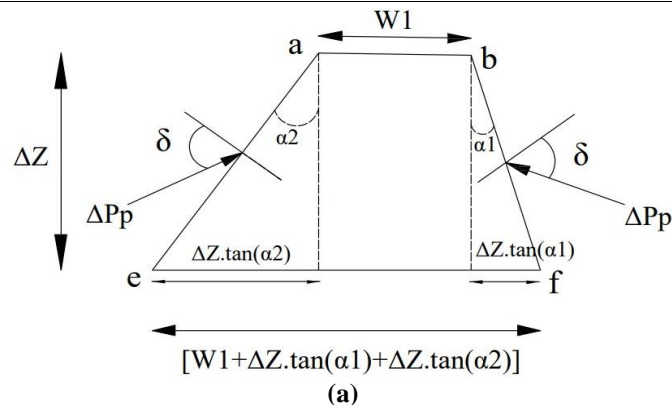
Fig. 2. Stress distribution under inclined loading

Table 1. Variation of load spread angle with thickness ratio and load inclination at different embedment ratio

H/W	θ (Deg.)	φ ₂ / φ ₁	α at D/W=0			α at D/W=1			α at D/W=2		
			α ₀₁	α ₀₂	α ₀₃	α ₁₁	α ₁₂	α ₁₃	α ₂₁	α ₂₂	α ₂₃
0.0	0	0.756	37	37	15	12	12	12	11	11	11
0.5			32	32	12	10	10	11	10.5	10.5	10
1.0			28	28	10	8	8	9	10	10	9
1.5			32	32	11	7	7	8	9	9	9
2.0			35	35	12	13	13	11	11	11	10
0.0			5	0.761	20	46	14	8	19	13	7
0.5	17	43			12	5	18	11	5.5	14	9
1.0	14	41			11	4	10	10	4	12	8
1.5	12	37			12	3	15	10	3	11	7.5
2.0	27	40			13	6	16	12	5	12	10
0.0	10	0.767			5	61	12	-4	26	13	-4
0.5			2	57	10	-3.5	18	11	-2	17.5	11
1.0			-1	51	9.5	-3	16	10	0	15	10
1.5			-4	48	9	0	19	12	2	17.5	11
2.0			-5	43	9	1	27	12.5	3	21	12
0.0			15	0.772	-32	72	13	-10	31	12	-10
0.5	-29	64			12	-8	29	11	-9	27	10
1.0	-24	57			11	-5	27	10	-8.5	23	10
1.5	-20	51			9	-2	24	9	-10	26	10
2.0	-29	62			10	-4	33	13	-11	30	11
0.0	20	0.777			-54	81	14	-21	45	12	-17.5
0.5			-52	73	12	-19	41	10	-15	33.5	13
1.0			-45	71	11	-15	38	9	-12.5	30	10
1.5			-48	73	12	-18	43	11	-13	32.3	11.5
2.0			-53	80	13	-20	47	12	-13.5	37	13
0.0			25	0.782	-70	90	14	-32	57	14	-26
0.5	-60	90			13	-29	51	12	-23	48	14
1.0	-58	90			10	-28	47	11	-22	37	12
1.5	-69	90			12	-24	43	12	-17.5	45	13
2.0	-69	90			13	-29	54	15	-20	56	14
0.0	30	0.756			-80	90	14	-42	74	13	-40
0.5			-75	90	13	-34	61	10	-37	56	12
1.0			-69	90	11	-29	55	10	-26	49	9
1.5			-68	90	10	-30	58	11	-28	55	11
2.0			-71	90	13	-44	75	12.5	-33	59	13

Table 2. Comparison of results with finite element analysis

H/W	D/W	ϕ_1, ϕ_2 (Degree)	Dimensionless bearing capacity ($q_{ult}/\gamma_1 W$)					
			$\theta = 0^\circ$		$\theta = 15^\circ$		$\theta = 30^\circ$	
			Present equation	F.E.M. analysis	Present equation	F.E.M. analysis	Present equation	F.E.M. analysis
0.00			7.50	10.21	1.99	6.78	0.008	1.025
0.50			21.93	14.06	11.53	8.72	3.74	5.14
1.00	0	41,31	39.88	21.27	20.91	13.84	3.74	9.75
1.50			51.99	33.47	20.91	16.42	3.74	9.75
2.00			51.99	38.18	20.91	22.44	3.74	9.75
0.00			11.01	15.48	3.27	9.59	0.09	5.00
0.50			30.39	25.67	16.09	12.91	7.08	7.69
1.00	0	43,33	54.32	53.91	31.53	20.07	7.28	12.33
1.50			79.69	85.91	33.78	26.67	7.28	17.43
2.00			79.69	91.97	33.78	40.27	7.28	17.43
0.00			19.27	29.77	6.55	14.82	0.53	6.20
0.50			49.84	53.88	26.58	28.39	11.55	12.28
1.00	0	46,36	87.82	102.45	50.54	49.83	18.5	18.48
1.50			130.75	159.29	69.47	74.75	18.5	28.72
2.00			152.98	167.29	69.47	97.79	18.5	28.72
0.00			37.34	44.25	22.15	33.83	12.68	17.66
0.50			67.93	65.93	40.99	51.88	22.73	23.75
1.00	1	41,31	100.49	85.78	60.28	60.22	31.91	34.83
1.50			134.55	140.33	79.84	69.52	40.78	45.12
2.00			170.02	157.52	99.62	93.39	49.51	56.81
0.00			51.61	52.72	30.66	37.85	17.25	21.19
0.50			92.62	83.49	55.54	60.04	30.21	34.78
1.00	1	43,33	136.44	131.39	81.08	77.99	42.15	44.83
1.50			182.38	177.51	106.98	108.87	53.72	58.93
2.00			226.24	218.28	132.47	138.62	65.83	74.29
0.00			83.44	91.34	49.78	46.11	27.47	34.67
0.50			149.43	156.93	88.64	76.57	46.71	52.34
1.00	1	46,36	220.45	234.01	128.73	125.11	64.66	70.47
1.50			295.30	358.29	169.46	177.29	82.06	97.99
2.00			373.65	410.80	210.70	220.67	99.23	125.70
0.00			75.75	74.29	48.25	63.03	29.16	46.78
0.50			122.53	98.60	76.81	76.55	45.29	56.14
1.00	2	41,31	168.91	153.45	104.51	104.96	59.94	68.16
1.50			214.69	198.50	131.40	145.21	73.49	79.11
2.00			259.30	244.65	157.35	175.46	86.26	97.39
0.00			104.21	83.72	66.38	70.38	39.74	56.78
0.50			166.61	131.40	103.60	93.37	59.63	66.63
1.00	2	43,33	228.48	201.40	139.57	152.09	77.48	85.68
1.50			289.44	251.91	174.30	171.05	93.93	111.60
2.00			348.52	338.19	207.60	199.77	109.41	131.39
0.00			167.43	131.44	106.76	115.93	63.23	80.16
0.50			268.016	252.68	164.41	146.52	91.21	100.64
1.00	2	46,36	367.92	384.29	219.82	233.96	116.00	128.52
1.50			466.24	508.37	272.96	321.40	138.85	157.46
2.00			561.00	659.83	323.48	412.34	160.47	218.31



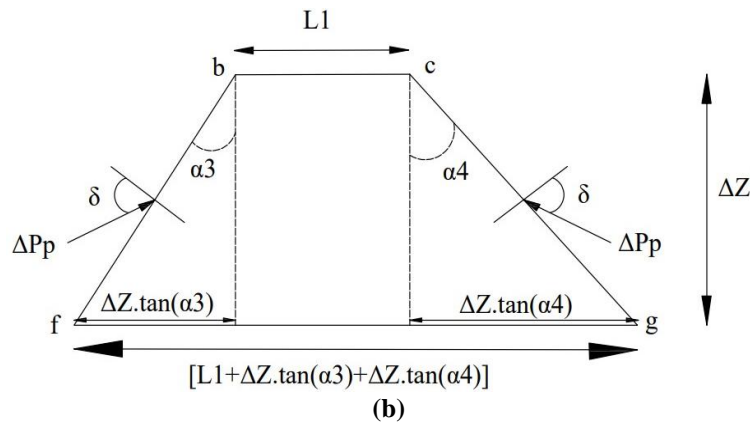


Fig. 3. Free body diagram across the footing (a) width (b) length

Summation of all the forces in the vertical direction for a small strip of thickness (ΔZ) leads to Eq. (1).

$$\begin{aligned} \sum F_V = 0 \\ \sigma_v \cdot \cos(\theta) \cdot (L1 \cdot W1) + \gamma_1 \cdot \left(\frac{\Delta Z}{3}\right) \cdot \\ \left\{ [W1 + \Delta Z \cdot \tan(\alpha1) + \Delta Z \cdot \tan(\alpha2)] \cdot [L1 \right. \\ \left. + \Delta Z \cdot \tan(\alpha3) + \Delta Z \cdot \tan(\alpha4)] + (L1 \cdot W1) \right. \\ \left. + \sqrt{\frac{(L1 \cdot W1) \cdot [W1 + \Delta Z \cdot \tan(\alpha1) + \Delta Z \cdot \tan(\alpha2)] \cdot [L1 + \Delta Z \cdot \tan(\alpha3) + \Delta Z \cdot \tan(\alpha4)]}{(L1 \cdot W1) \cdot [L1 + \Delta Z \cdot \tan(\alpha3) + \Delta Z \cdot \tan(\alpha4)]}} \right\} \\ - \Delta P_{pv} - (\sigma_v + \Delta \sigma_v) \cdot \cos(\theta) \cdot [W1 + \Delta Z \cdot \tan(\alpha1) + \Delta Z \cdot \tan(\alpha2)] \cdot [L1 + \Delta Z \cdot \tan(\alpha3) + \Delta Z \cdot \tan(\alpha4)] = 0 \end{aligned} \quad (1)$$

where γ_I : is the unit weight of the upper dense sand layer, and σ_v and ΔP_{pv} : are the vertical component of applied stress and the passive pressure, respectively. It worth noting here that the passive pressure on all sides of the projected area is not equal, however, following Meyerhof and Hanna (1978), it was assumed to be the same in this analysis. The passive pressure (ΔP_{pv}) in the vertical direction can be written as:

$$\Delta P_{pv} = \Delta P_p \cdot \sin(\delta) \quad (2)$$

$$\begin{aligned} \Delta P_{pv} = \gamma_1 \cdot K_p \cdot \left(D + Z \right. \\ \left. + \frac{\Delta Z}{2} \right) \cdot \Delta Z \cdot [2L1 \\ + 2W1 \\ + \Delta Z \cdot \tan(\alpha1) \\ + \Delta Z \cdot \tan(\alpha2) \\ + \Delta Z \cdot \tan(\alpha3) \\ + \Delta Z \cdot \tan(\alpha4)] \cdot \sin(\delta) \end{aligned} \quad (3)$$

in which K_p : depends upon the product of passive earth pressure coefficient as per Caquot and Kerisel (1949) and punching shear inclination factor as per Meyerhof and Hanna (1978).

Rewriting the Eq. (1):

$$\begin{aligned} \sigma_v \cdot \cos(\theta) \cdot (L1 \cdot W1) \\ + \gamma_1 \cdot \left(\frac{\Delta Z}{3}\right) \cdot \\ \left\{ \begin{aligned} &(L1 \cdot W1) + \\ &W1 \cdot [(\Delta Z \cdot \tan(\alpha3) + \Delta Z \cdot \tan(\alpha4))] \\ &+ L1 \cdot [(\Delta Z \cdot \tan(\alpha1) + \Delta Z \cdot \tan(\alpha2))] \\ &+ \Delta Z^2 \cdot \left[\begin{aligned} &\tan(\alpha1) \cdot \tan(\alpha3) + \\ &\tan(\alpha1) \cdot \tan(\alpha4) + \\ &\tan(\alpha2) \cdot \tan(\alpha3) + \\ &\tan(\alpha2) \cdot \tan(\alpha4) \end{aligned} \right] \end{aligned} \right\} \\ \left\{ \begin{aligned} &(L1 \cdot W1) \cdot \left[\begin{aligned} &L1 \cdot W1 + \\ &W1 \cdot [(\Delta Z \cdot \tan(\alpha3) + \Delta Z \cdot \tan(\alpha4))] \\ &+ L1 \cdot [(\Delta Z \cdot \tan(\alpha1) + \Delta Z \cdot \tan(\alpha2))] \\ &+ \Delta Z^2 \cdot \left[\begin{aligned} &\tan(\alpha1) \cdot \tan(\alpha3) + \\ &\tan(\alpha1) \cdot \tan(\alpha4) + \\ &\tan(\alpha2) \cdot \tan(\alpha3) + \\ &\tan(\alpha2) \cdot \tan(\alpha4) \end{aligned} \right] \end{aligned} \right\} \\ - \Delta P_{pv} \\ - (\sigma_v + \Delta \sigma_v) \cdot \cos(\theta) \cdot \\ \left\{ \begin{aligned} &(L1 \cdot W1) + W1 \cdot [\Delta Z \cdot \tan(\alpha3) + \Delta Z \cdot \tan(\alpha4)] \\ &+ L1 \cdot [\Delta Z \cdot \tan(\alpha1) + \Delta Z \cdot \tan(\alpha2)] + \\ &\Delta Z^2 \cdot \left[\begin{aligned} &\tan(\alpha1) \cdot \tan(\alpha3) + \tan(\alpha1) \cdot \tan(\alpha4) \\ &+ \tan(\alpha2) \cdot \tan(\alpha3) + \tan(\alpha2) \cdot \tan(\alpha4) \end{aligned} \right] \end{aligned} \right\} \end{aligned} \quad (4)$$

Since ΔZ and $\Delta \sigma_v$ are very small, so their square or their product would be also very small. Thus neglecting the terms such as $\left(\frac{\Delta Z^2}{3} \cdot \tan(\alpha1) \cdot \tan(\alpha3)\right)$, $\frac{\Delta Z^2}{3} \cdot \tan(\alpha2) \cdot \tan(\alpha4)$, $(\sigma_v + \Delta \sigma_v) \cdot \cos(\theta) \cdot \Delta Z \cdot \tan(\alpha3)$, $(\sigma_v + \Delta \sigma_v) \cdot \cos(\theta) \cdot \Delta Z^2 \cdot \tan(\alpha1) \cdot \tan(\alpha3)$ etc...

Eq. (5) is obtained.

$$\begin{aligned} & \sigma_v \cdot \cos(\theta) \cdot (L1 \cdot W1) + \\ & \gamma_1 \cdot \left(\frac{\Delta Z}{3}\right) \cdot [2(L1 \cdot W1) + (L1 \cdot W1)] - \\ & \Delta P_{pv} - \\ & (\sigma_v + \Delta \sigma_v) \cdot \cos(\theta) \cdot (L1 \cdot W1) = 0 \end{aligned} \quad (5)$$

Similarly, neglecting the terms such as $\frac{1}{2} \cdot [(2W1 + 2L1) \cdot \Delta Z^2 + \Delta Z^3 \cdot [\tan(\alpha1) + \tan(\alpha2) + \tan(\alpha3) + \tan(\alpha4)]]$ after expanding the Eq. (3), because $\Delta Z^2, \Delta Z^3$ are very small, results in new Eq. (6).

$$\Delta P_{pv} = 2\gamma_1 \cdot K_p \cdot (D + Z) \cdot (L1 + W1) \cdot \Delta Z \cdot \sin(\delta) \quad (6)$$

Eq. (7) is obtained by substituting the ΔP_{pv} in Eq. (5).

$$\begin{aligned} & \sigma_v \cdot \cos(\theta) \cdot (L1 \cdot W1) + \\ & \gamma_1 \cdot \left(\frac{\Delta Z}{3}\right) \cdot [3(L1 \cdot W1)] - 2\gamma_1 \cdot K_p \cdot (D + \\ & Z) \cdot (L1 + W1) \cdot \Delta Z \cdot \sin(\delta) - (\sigma_v + \\ & \Delta \sigma_v) \cdot \cos(\theta) \cdot (L1 \cdot W1) = 0 \end{aligned} \quad (7)$$

Simplification of Eq. (7) leads to Eq. (8).

$$\begin{aligned} & \Delta \sigma_v \cdot \cos(\theta) \cdot (L1 \cdot W1) = \\ & \gamma_1 \cdot [(L1 \cdot W1) - 2K_p \cdot (D + Z) \cdot (L1 + \\ & W1) \cdot \sin(\delta)] \cdot \Delta Z \end{aligned} \quad (8)$$

Dividing Eq. (8) on both sides with $(W1 \cdot L1)$ results in Eq. (9).

$$\Delta \sigma_v \cdot \cos(\theta) = \gamma_1 \cdot \left[1 - \frac{2K_p \cdot (D + Z) \cdot (L1 + W1) \cdot \sin(\delta)}{(L1 \cdot W1)}\right] \cdot \Delta Z \quad (9)$$

Integrating Eq. (9) as shown in Eq. (10) on both sides, results in Eq. (11).

$$\begin{aligned} & \int \Delta \sigma_v \cdot \cos(\theta) \\ & = \int \gamma_1 \cdot \left[1 - \frac{2K_p \cdot (D + Z) \cdot (L1 + W1) \cdot \sin(\delta)}{(L1 \cdot W1)}\right] \cdot \Delta Z \end{aligned} \quad (10)$$

$$\Delta \sigma_v \cdot \cos(\theta) = \gamma_1 \cdot Z - \left[\frac{2\gamma_1 \cdot K_p \cdot (D \cdot Z + \frac{Z^2}{2}) \cdot (L1 + W1) \cdot \sin(\delta)}{(L1 \cdot W1)} \right] + C \quad (11)$$

where C : is constant of integration.

In order to find C , the following boundary conditions are applied to Eq. (11). At $Z = 0$, $L1 = L$, $W1 = W$ and $\sigma_v = q_u$, which results in Eq. (12).

$$C = q_u \cdot \cos(\theta) \quad (12)$$

where q_u : is the ultimate load bearing capacity of the rectangular footing in the layered sand.

Further, at $Z = H$, $L1 = [L + H \cdot \tan(\alpha3) + H \cdot \tan(\alpha4)]$, $W1 = [W + H \cdot \tan(\alpha1) + H \cdot \tan(\alpha2)]$ and $\sigma_v = q_L$, will result into Eq. (13) is obtained from Eq. (11).

$$\begin{aligned} & q_L \cdot \cos(\theta) = \gamma_1 \cdot H \\ & - \left\{ \frac{2\gamma_1 \cdot K_p \cdot H \cdot \left(D + \frac{H}{2}\right) \cdot \left[\frac{[(W + H \cdot \tan(\alpha1) + H \cdot \tan(\alpha2))] \cdot \sin(\delta)}{[L + H \cdot \tan(\alpha3) + H \cdot \tan(\alpha4)]} \right]}{[W + H \cdot \tan(\alpha1) + H \cdot \tan(\alpha2)] \cdot [L + H \cdot \tan(\alpha3) + H \cdot \tan(\alpha4)]} \right\} \\ & + q_u \cdot \cos(\theta) \end{aligned} \quad (13)$$

where q_L : is the bearing capacity of the lower loose sand layer, $q_L \cdot \cos(\theta)$ and $q_u \cdot \cos(\theta)$: is the vertical component of the bearing capacity q_L and q_u which were further designated as q_{Lv} and q_{uv} , respectively in this derivation. As per IS 6403 (1981), for the sand under inclined loading, the bearing capacity is given by Eq. (14).

$$\begin{aligned} & q_{Lv} = \gamma_1 \cdot (D + \\ & H) \cdot N_{q2} \cdot S_{q2} \cdot d_{q2} \cdot i_{q2} + \\ & \left(\frac{1}{2}\right) \cdot (\gamma_2 \cdot W \cdot N_{\gamma2} \cdot S_{\gamma2} \cdot d_{\gamma2} \cdot i_{\gamma2}) \end{aligned} \quad (14)$$

where d_{q2} , $d_{\gamma2}$, i_{q2} , $i_{\gamma2}$ and S_{q2} , $S_{\gamma2}$: are the depth, inclination and shape factors. The equation for the inclination and shape factors are given in Eqs. (15a) and (15b) and Eqs. (16a) and (16b), respectively.

$$i_{q2} = \left(1 - \frac{\theta}{90^\circ}\right)^2 \quad (15a)$$

$$i_{\gamma2} = \left(1 - \frac{\theta}{\varphi_2}\right)^2 \quad (15b)$$

and

$$S_{q2} = \left(1 + \frac{0.2W}{L}\right) \tag{16a}$$

$$S_{\gamma2} = \left(1 - \frac{0.4W}{L}\right) \tag{16b}$$

Substituting Eqs. (14, 15a, 15b, 16a and 16b) in Eq. (13) and after rearranging it, Eq. (17) is resulted.

$$q_{uv} = \left[\gamma_1 \cdot \left(1 + \frac{0.2W}{L}\right) \cdot (D + H) \cdot N_{q2} \cdot d_{q2} \cdot i_{q2} \right] + \left[\left(\frac{1}{2}\right) \cdot \left(1 - \frac{0.4W}{L}\right) \cdot \gamma_2 \cdot W \cdot N_{\gamma2} \cdot d_{\gamma2} \cdot i_{\gamma2} \right] - \gamma_1 \cdot H + \left\{ \frac{2\gamma_1 \cdot K_p \cdot H \cdot \left(D + \frac{H}{2}\right) \cdot \left[\frac{W + L + H \cdot \tan(\alpha1) + H \cdot \tan(\alpha2)}{H \cdot \tan(\alpha3) + H \cdot \tan(\alpha4)} \right] \cdot \sin(\delta)}{[W + H \cdot \tan(\alpha1) + H \cdot \tan(\alpha2)] \cdot [L + H \cdot \tan(\alpha3) + H \cdot \tan(\alpha4)]} \right\} \tag{17}$$

Further, by simplification of Eq. (17), Eq. (18) is obtained.

$$(q_{uv}) = (\gamma_1) \cdot (N_{\gamma2}) \cdot \left[\left(1 + \frac{0.2W}{L}\right) \cdot (D + H) \cdot \left(\frac{N_{q2}}{N_{\gamma2}}\right) \cdot d_{q2} \cdot i_{q2} + \left(\frac{1}{2}\right) \cdot \left(\frac{\gamma_2}{\gamma_1}\right) \cdot \left(1 - \frac{0.4W}{L}\right) \cdot W \cdot d_{\gamma2} \cdot i_{\gamma2} \right] - \gamma_1 \cdot H + \left\{ \frac{2\gamma_1 \cdot K_p \cdot H \cdot \left(D + \frac{H}{2}\right) \cdot \left[\frac{W + L + H \cdot \tan(\alpha1) + H \cdot \tan(\alpha2)}{H \cdot \tan(\alpha3) + H \cdot \tan(\alpha4)} \right] \cdot \sin(\delta)}{[W + H \cdot \tan(\alpha1) + H \cdot \tan(\alpha2)] \cdot [L + H \cdot \tan(\alpha3) + H \cdot \tan(\alpha4)]} \right\} \tag{18}$$

To convert Eq. (18) into a dimensionless form, it is divided with $\gamma_1 W$ on both sides. Then Eq. (19) is obtained.

$$\left(\frac{q_{uv}}{\gamma_1 W}\right) = \left(\frac{\gamma_2}{\gamma_1}\right) \cdot (N_{\gamma2}) \cdot \left[\left(\frac{\gamma_1}{\gamma_2}\right) \cdot \left(1 + \frac{0.2W}{L}\right) \cdot \left(\frac{D}{W}\right) + \frac{H}{W} \cdot \left(\frac{N_{q2}}{N_{\gamma2}}\right) \cdot d_{q2} \cdot i_{q2} + \left(\frac{1}{2}\right) \cdot \left(1 - \frac{0.4W}{L}\right) \cdot d_{\gamma2} \cdot i_{\gamma2} \right] - \left(\frac{H}{W}\right) + \left\{ \frac{2K_p \cdot \left(\frac{H}{W}\right) \cdot \left[1 + \left(\frac{L}{W}\right) + \left(\frac{H}{W}\right) \cdot \left[\frac{\tan(\alpha1) + \tan(\alpha2)}{[\tan(\alpha3) + \tan(\alpha4)]} \right] \right] \cdot \left(\frac{D}{W} + \frac{H}{2W}\right) \cdot \sin(\delta)}{\left\{ \left(\frac{H}{W}\right) \cdot \left[\frac{1 + \left(\frac{H}{W}\right)}{[\tan(\alpha1) + \tan(\alpha2)]} \right] \right\} \cdot \left\{ \left(\frac{L}{W}\right) + \left(\frac{H}{W}\right) \cdot \left[\frac{1}{[\tan(\alpha3) + \tan(\alpha4)]} \right] \right\}} \right\} \leq q_t \tag{19}$$

The dimensionless ultimate bearing capacity ($q_{uv}/\gamma_1 W$) derived as per Eq. (19) is valid only up to the bearing capacity of the upper sand layer (q_t), after which bearing capacity remains constant and was primarily dependent on the upper dense sand layer. Further, from Eq. (19), the bearing capacity of rectangular footing on layered sand under inclined load depends on: 1) Embedment depth of footing (D); 2) Thickness of dense sand layer (H); 3) Unit weight and friction angle of the upper dense (γ_1, ϕ_1) and lower loose (γ_2, ϕ_2) sand layer; 4) Dimensions of the footing (L and W); and 5) Load inclination (θ) with respect to vertical. It is pertinent to mention here that the angle $\alpha1, \alpha2, \alpha3$ and $\alpha4$ associated with the load spread mechanism too depends on the above parameters. For strip and circular footings, the angles $\alpha1$ and $\alpha2$ were both considered equal to the inclination of the applied load in the work of Meyerhof and

Hanna (1978). In the present study, to have a reasonable estimate of bearing capacity using the limit equilibrium methodology, the magnitude of the all load spread angles were determined for surface ($\alpha_1, \alpha_2, \alpha_3, \alpha_4$) as well as for embedment ratio (D/W) of 1 ($\alpha_{11}, \alpha_{12}, \alpha_{13}, \alpha_{14}$) and 2 ($\alpha_{21}, \alpha_{22}, \alpha_{23}, \alpha_{24}$), respectively by performing Finite Element analysis in the ABAQUS software using C3D8R element. For the numerical study, the load inclination angle (θ) was varied from 0° to 30° at an interval of 5° . The impact of soil density was considered in the analysis. The relation between the unit weights and friction angles used for modelling were considered as per Bowles (1977) for the upper dense and the lower loose sand layer and are shown in Tables 3 and 4, respectively.

It is pertinent to mention here that Dawarci et al. (2014) reported a friction angle of 36° and 42° for the sand corresponding to a unit weight of 15.44 kN/m^3 and 16.65 kN/m^3 , respectively. Khatri et al. (2017b) obtained a friction angle of sand as 33.4° corresponding to a unit weight of 13.87 kN/m^3 . Das et al. (2021) used a friction angle for the loose (31° - 36°) and dense (41° - 46°) sand for performing the numerical study of the ring footing on layered sand. Furthermore, Hanna (1981) and Farah (2004) used a punching shearing mechanism to acquire the bearing capacity of the strip footing on layered soil, obtaining a friction angle of 47.7° and 34° , respectively, corresponding to a unit weight of 16.33 kN/m^3 and 13.78 kN/m^3 . Given the foregoing, the mechanism, as well as the unit weights and friction angles (Tables 3 and 4) selected for modelling, are justified.

Further, for the numerical study, the dilation angles for the upper dense and lower loose sand layers were calculated as per Szypcio and Dołżyk (2006). Modulus of elasticity for the upper dense and lower loose sand layers were derived from $1200(N+6) \text{ kPa}$ as per El-Kasaby (1991). The standard penetration resistance (N) was

calculated as per IS 6403 (1981) corresponding to the friction angles for the upper dense and lower loose sand layers used for modelling. Numerical study was conducted for different thickness ratio (H/W) which were varied from 0.00 to 2.00. More details of the numerical study can be seen in Panwar and Dutta (2021). It is pertinent mention here that the Finite Element analysis was performed both for the surface and embedded footing.

Figure 4 shows the failure surface movement with the variation in load inclination in the form of vectorial displacement at different embedment ratio. The failure surface of the rectangular footing resting on upper dense sand overlying lower loose sand under inclined load was observed to make different angles α_1 and α_2 across the width, but angles α_3 and α_4 were found to be the same across the length for surface as well as for embedded footing. Figures 5a and 5b shows the load spread angle α_1 , α_2 and α_3 across the width and length of the rectangular footing. All the load spread angles were measured with respect to the vertical axis below the base edges of the rectangular footing in the direction of load inclination as well as in the opposite direction as shown in the Figure 5.

Table 1 shows the variation of the load spread angle with the thickness ratio (H/W) load inclination (θ) and soil friction ratio (ϕ_2/ϕ_1) at different embedment ratio (D/W). From the present study, for surface footing ($D/W = 0$) it was observed that with the increase in the thickness ratio, all the load spread angles were found to decrease as long as the bearing capacity was dependent on the properties of both the sand layers. But when the failure surface confined to the upper dense sand layer, all load spread angles were observed to increase for each load inclination. Similar behaviour observed when the embedment ratio increased from 1 to 2. It is pertinent to mention here that the sign convention for the α_1 was considered negative when measured towards left of the vertical axis otherwise it was considered positive. As the

soil defining parameters changed, there was change in all load spread angles. Load spread angle variation with thickness ratio, load inclination and soil friction ratio were presented both for the surface and embedded footing through Eqs. (20(a-c), 21(a-c) and 22(a-c)).

For surface footing ($D/W = 0$),

$$\alpha_{01} = -3.45 * \left(\frac{H}{W}\right) - 3.69 * (\theta) - 137.53 * \left(\frac{\varphi_2}{\varphi_1}\right) + 139.78 \quad (20a)$$

$$\alpha_{02} = \exp * \left(-0.036 * \left(\frac{H}{W}\right) + 0.033 * (\theta) + 1.77 * \left(\frac{\varphi_2}{\varphi_1}\right) + 2.23\right) \quad (20b)$$

$$\alpha_{03} = \alpha_{04} = -1.24 * \left(\frac{H}{W}\right) + 0.04 * (\theta) + 12.58 \quad (20c)$$

For embedded footing ($D/W = 1$),

$$\alpha_{11} = \left[\left(-0.10 * \left(\frac{H}{W}\right)^3 - (0.051 * (\theta)^2) - \left(114.64 * \left(\frac{\varphi_2}{\varphi_1}\right)\right) + 94.20 \right) \right] \quad (21a)$$

$$\alpha_{12} = \exp * \left(0.072 * \left(\frac{H}{W}\right) + 0.057 * (\theta) - 0.32 * \left(\frac{\varphi_2}{\varphi_1}\right) + 2.72\right) \quad (21b)$$

$$\alpha_{13} = \alpha_{14} = -0.85 * \left(\frac{H}{W}\right) + 0.08 * (\theta) + 11.23 \quad (21c)$$

For embedded footing ($D/W = 2$),

$$\alpha_{21} = \left[\left(0.21 * \left(\frac{H}{W}\right)^3 - ((0.043 * (\theta)^2)) - \left(206.50 * \left(\frac{\varphi_2}{\varphi_1}\right)\right) + 163.33 \right) \right] \quad (22a)$$

$$\alpha_{22} = \exp * \left(0.061 * \left(\frac{H}{W}\right) + 0.055 * (\theta) + 4.85 * \left(\frac{\varphi_2}{\varphi_1}\right) - 1.42\right) \quad (22b)$$

$$\alpha_{23} = \alpha_{24} = -0.80 * \left(\frac{H}{W}\right) + 0.02 * (\theta) + 138.27 * \left(\frac{\varphi_2}{\varphi_1}\right) - 94.63 \quad (22c)$$

Table 3. Upper dense sand layer properties used for modelling

φ_1	γ_1 (kN/m ³)
41°	19.5
42°	20.0
43°	20.5
44°	21.0
45°	21.5
46°	22.0

Table 4. Lower loose sand layer properties used for modelling

φ_2	γ_2 (kN/m ³)
31°	14.5
32°	15.0
33°	15.5
34°	16.0
35°	16.5
36°	17.0

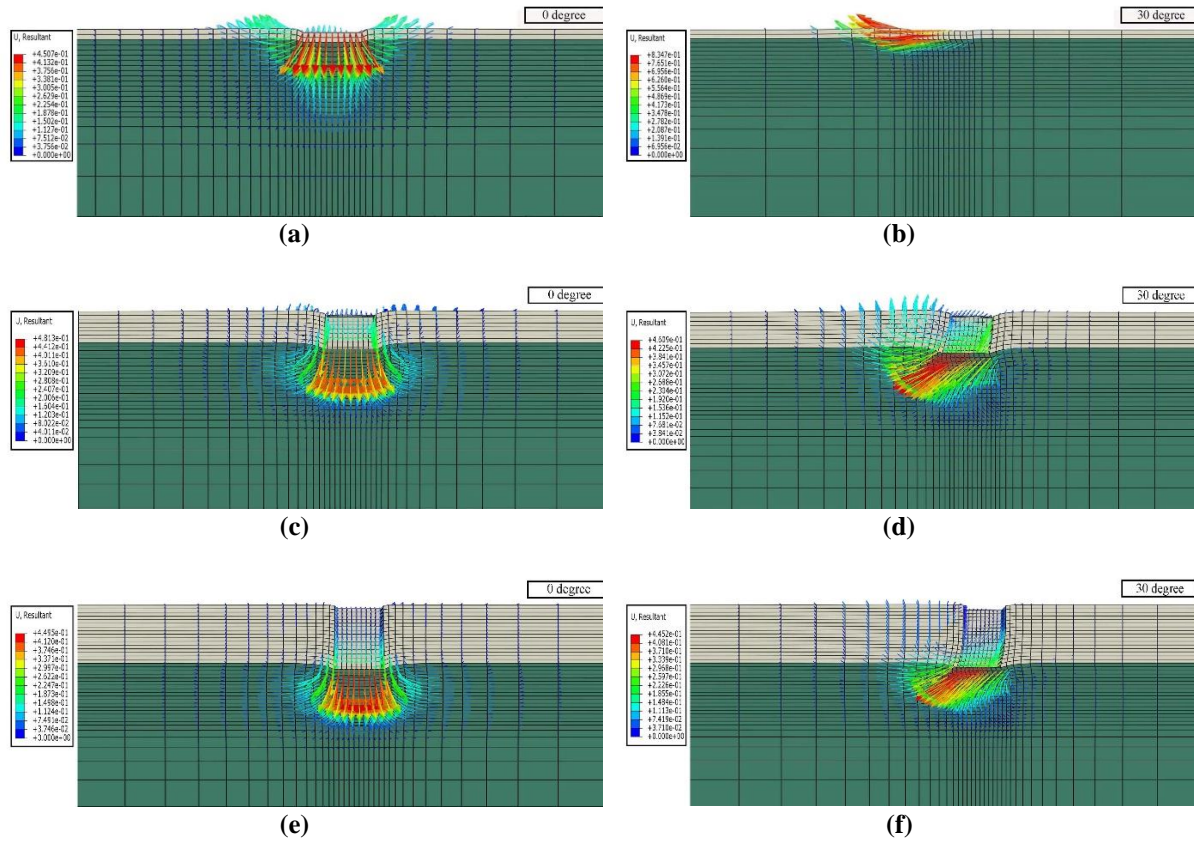


Fig. 4. Vectorial displacement failure: a) and b) For surface footing; c) and d) For embedment ratio 1; and e) and f) For embedment ratio 2 under a load inclination of 0° and 30°

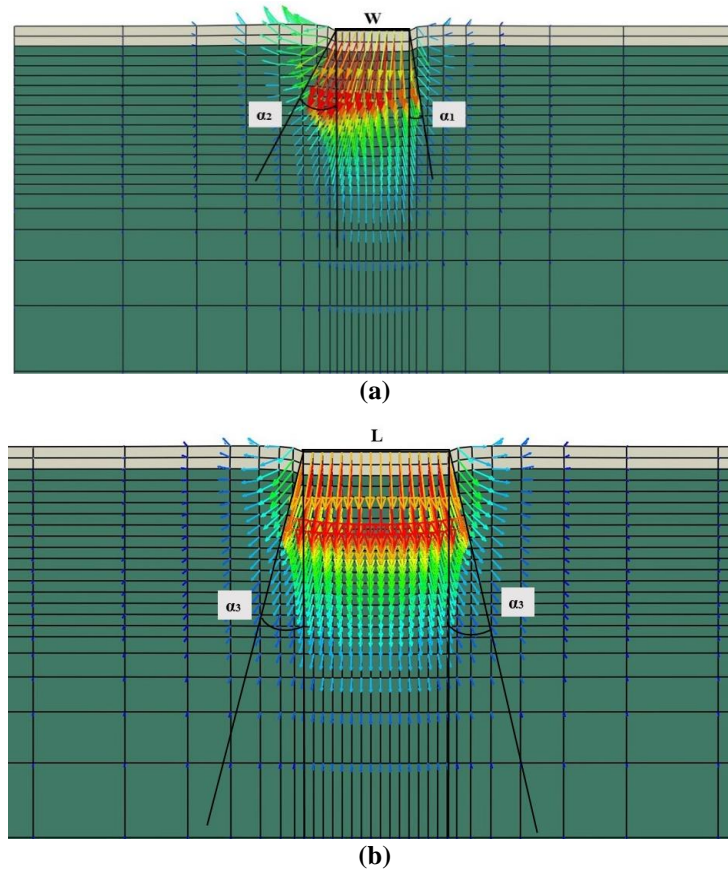


Fig. 5. Load spread angle across the: a) Width (W); and b) Length (L) of the footing

3. Validation with the FEM Results

Numerical study was performed as per Panwar and Dutta (2021) for the calculation of load spread angle α_1 , α_2 , α_3 , and α_4 for the surface ($D/W = 0$) and embedded ($D/W = 1$ and 2) footing. The proposed Eq. (19) also depends on these loads spread angles. A validation of the proposed equation with the numerical study was performed corresponding to varying thickness ratio (0.00 to 2.00), load inclination (0° to 30°) and friction angles of upper dense (41° to 46°) and lower loose (31° to 36°) sand layers under the inclined load. Comparison of the results was tabulated in Table 2 for the specific parameter of the friction angles, thickness ratio and load inclination at different embedment ratio.

Study of Table 2 reveals that when the load inclination increased from 0° to 30° , the results obtained from the proposed equation were in line with the results obtained from the finite element analysis. The overall average deviation was observed to increase with the increase in the embedment ratio and found to be 14.56%, 18.71% and 23.56% at an embedment ratio of 0, 1 and 2, respectively. This difference in the results is attributed to the use of passive earth pressure coefficient as per Caquot and Kerisel (1949) and punching shear inclination factors as per Meyerhof and Hanna (1978) in the derived Eq. (19). It is worth noting that the bearing capacity determined in the numerical study corresponded to a peak in the pressure relative settlement plot or determined using the double tangent method, whichever came first.

4. Results and Discussions

With the use of Eq. (19), the bearing capacity of rectangular footing on layered sand was calculated by varying the parameters such as thickness ratio (H/W), friction angle of sands, embedment ratio (D/W) and load inclination (θ). Further, the bearing capacity was expressed in a dimensionless form ($q_{uv}/\gamma_1 W$). The results

of this parametric study are described below.

4.1. Effect of Thickness Ratio, Sand Friction Angle and Embedment Ratio on the Dimensionless Bearing Capacity

In order to study the effect of the thickness ratio, sand friction angle and embedment ratio on the dimensionless bearing capacity, the results were plotted in Figure 6 corresponding to upper dense friction angle (41° and 46°) and lower loose sand (31° - 36°) layer friction angle at varying thickness ratio (0.25 to 2.00) for rectangular footing under vertical loading. Study of Figure 6a reveals that when thickness ratio increased from 0.00 to 2.00 for combination of the ϕ_1 (41°) and ϕ_2 (31° - 36°), there was an increase in the dimensionless bearing capacity. This may be due to the increase in the thickness of the upper dense sand layer. Further, study of Figure 6a reveals that with the increase in the thickness ratio, the dimensionless bearing capacity reached to the value of q_t (ultimate bearing capacity of upper dense sand) at a particular thickness ratio and becomes constant corresponding to the rest of the thickness ratio and similar behaviour observed in Figures 6b, 6c and 6e. This may be attributed to the fact that beyond a specific thickness ratio the failure surface remains in the upper dense sand and no contribution was observed of the lower loose sand layer beyond that specific thickness ratio. The trend was same corresponding to all ϕ_1 and ϕ_2 at varying thickness ratio.

Further, study of Figure 6 reveals that corresponding to $\phi_1 = 46^\circ$ and $\phi_2 = 31^\circ$, the dimensionless bearing capacity for surface footing obtained from the proposed equation for a thickness ratio of 0.00 was about 7.50 which increased to 26.27, 52.05 and 116.90 for a thickness ratio of 0.50, 1.00 and 2, respectively. It implies that the bearing capacity at a thickness ratio of 0.50, 1.00 and 2 was about 3.50, 6.94 and 15.58 times of its initial value. Figure 6 further reveals that with the increase in the friction

angle of upper dense sand layer from 41^0 to 46^0 , the dimensionless bearing capacity increased due to increase in the frictional resistance. A close examination of Figures 6c, 6d and 6e, 6f reveals that with the increase the embedment ratio (1 and 2), the dimensionless bearing capacity also increases. This may be due to increase in the additional surcharge load besides the increase in upper dense sand layer. The increase in the dimensionless bearing

capacity obtained from the proposed equation was 4.97 and 10.5 times the dimensionless bearing capacity of surface footing for an embedment ratio 1 and 2 respectively. Figure 6 further reveals that the highest and the lowest increase in the dimensionless bearing capacity was observed at a friction angle combination of 46^0 - 36^0 and 41^0 - 31^0 and at an embedment ratio 2 and 0 respectively at varying thickness ratio.

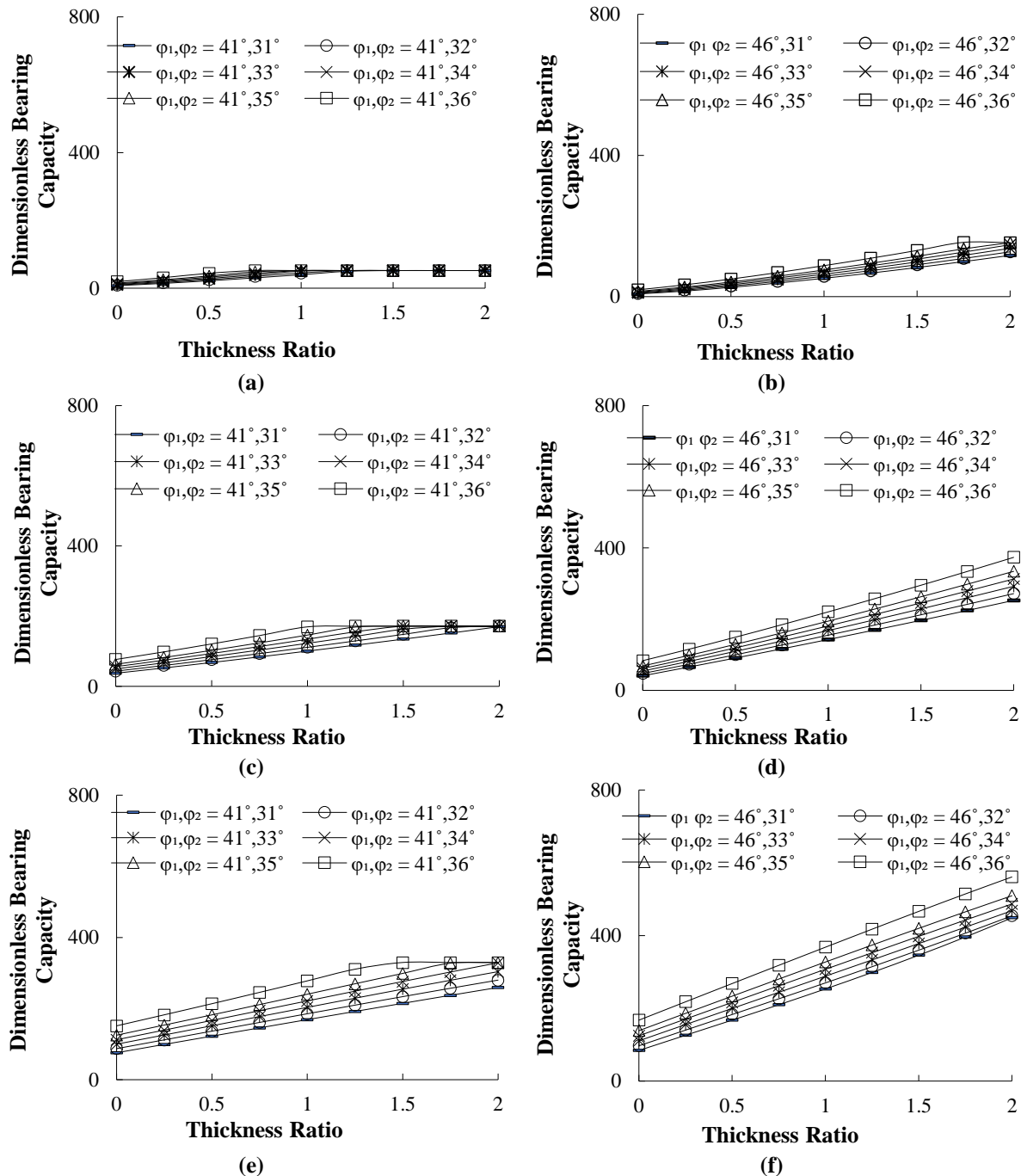
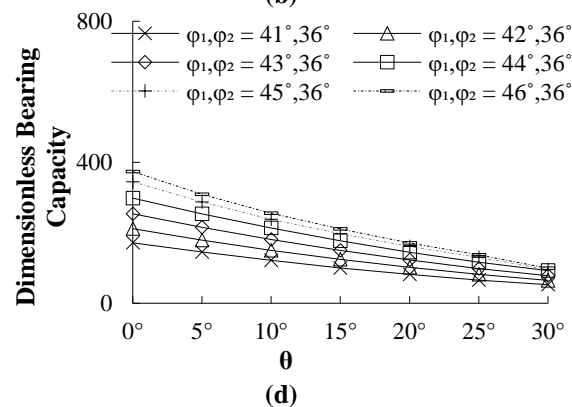
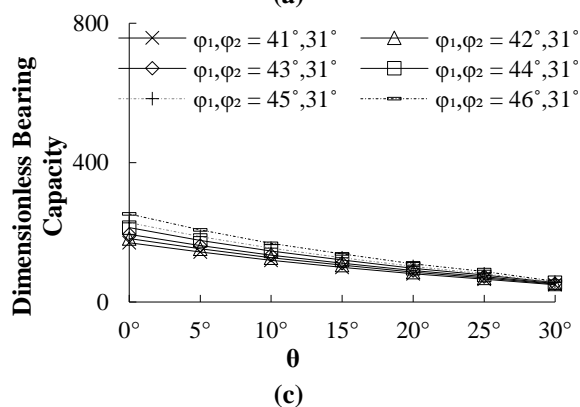
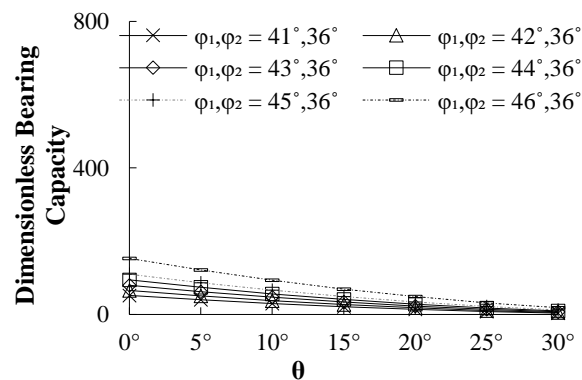
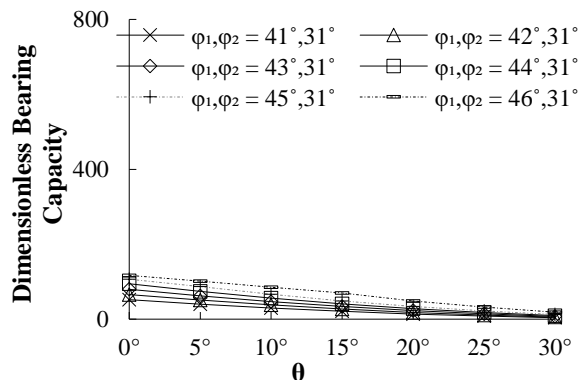


Fig. 6. Plot of dimensionless bearing capacity: a) and b) At $D/W = 0$; c) and d) At $D/W = 1$; and e) and f) At $D/W = 2$ with varying ϕ_1 (41^0 and 46^0) and ϕ_2 (31^0 - 36^0) at varying thickness ratio

4.2. Effect of Load Inclination and Embedment Ratio on the Dimensionless Bearing Capacity

In order to study the effect of the load inclination on the dimensionless bearing capacity, the results were plotted in Figure 7 corresponding to upper dense sand friction angle (41° to 46°) and lower loose sand layer friction angle (31 and 36°) at varying load inclination (0° to 30°) for specific thickness ratio ($H/W=2$) with the increase in embedment ratio (0 to 2). Study of Figures 7a, 7b reveals that at thickness ratio of 2, with the increase in the load inclination from 0° to 30° , there was decrease in the dimensionless bearing capacity for all friction angle combination and this may be due to the movement of the failure surface in the direction of load application. Also, the vertical and horizontal displacement found to decrease and increase respectively resulting failure of the footing. For $\varphi_1 = 46^{\circ}$ and $\varphi_2 = 36^{\circ}$ and at a thickness ratio of 2.00, the dimensionless bearing capacity of surface footing obtained from the proposed equation for a load inclination of 0° was about 152.98 which decreased to 121.53,

69.47 and 18.50 for a load inclination of 5° , 15° and 30° respectively. It implies that the dimensionless bearing capacity at a load inclination of 5° , 15° and 30° decreased about 20.55%, 54.58% and 87.90% of its initial value. Further study of Figures 7c, 7d 7e and 7f shows that as the embedment ratio increased from 0 to 1 and 2, the dimensionless bearing capacity increased but with a decreasing trend with the increase in the load inclination. This is attributed to the increase in the thickness of the upper dense sand layer and additional increase of surcharge load. Similar trend was observed at other thickness ratios as evident from Figure 7. The maximum decrease in the dimensionless bearing capacity obtained from the proposed equation was 99.89 %, 66.04 % and 61.5 % with the increase in the load inclination from 0° to 30° for an embedment ratio 0, 1 and 2, respectively. A close examination of Figure 7 reveals that highest and the lowest increase in the dimensionless bearing capacity was observed at embedment ratio (D/W) of 2.00 and 0, respectively for different friction angle and load inclination combinations.



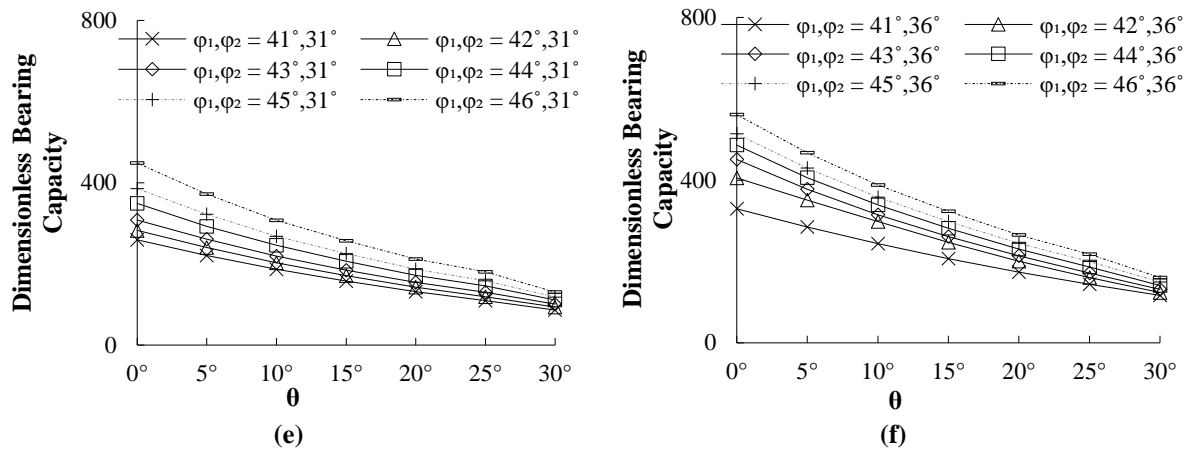
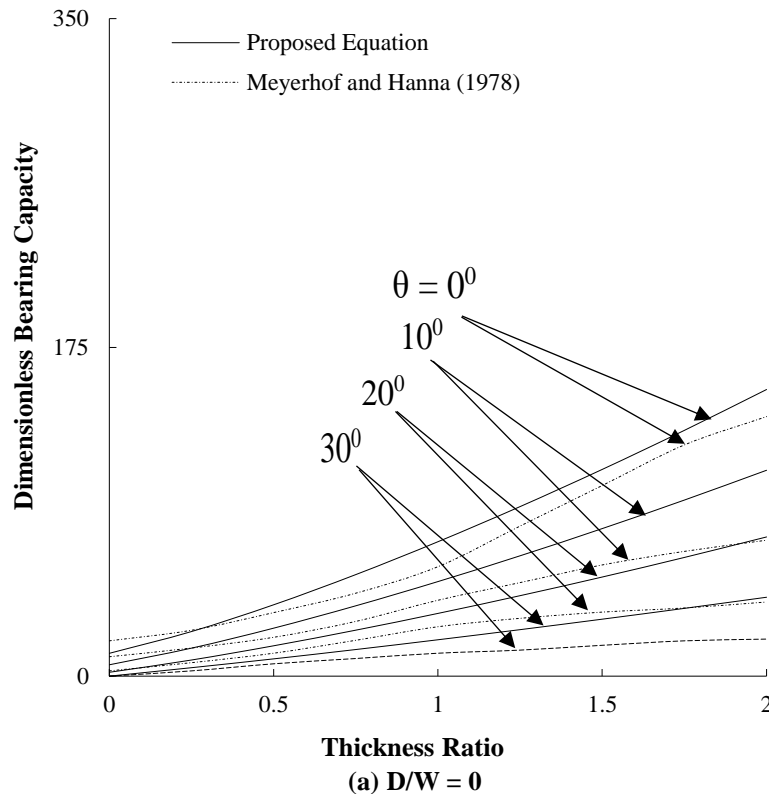


Fig. 7. Plot of dimensionless bearing capacity: a) and b) At $D/W = 0$; c) and d) at $D/W = 1$; and e) and f) At $D/W = 2$ with varying load inclination ($\theta = 0^\circ$ to 30°) for soil combination of ϕ_1 (41° - 46°) and ϕ_2 (31° and 36°) at some specific thickness ratio

4.3. Comparison

The experimental results reported by Meyerhof and Hanna (1978) were compared with the results obtained from the proposed Eq. (19). The dimensionless bearing capacity obtained from Eq. (19) for $L/W = 1$ was calculated and compared with the results reported by Meyerhof and Hanna (1978) for the circular footing as both the footings have similar shape factor. It is pertinent to mention here that Meyerhof and Hanna (1978) used the friction angle and unit weight of the upper dense and lower

loose sand layer as 47.5° and 34° , 16.33 kN/m^3 and 13.78 kN/m^3 , respectively. The comparison was shown in Figure 8 corresponding to a load inclination (θ) of 0° , 10° , 20° and 30° for varying thickness ratio (H/W) with embedment ratio (D/W) = 0 and 1. Study of Figure 8a reveals that for the surface footing, the results obtained from the proposed Eq. (19) at smaller thickness ratio were found to be conservative in comparison to the results of Meyerhof and Hanna (1978).



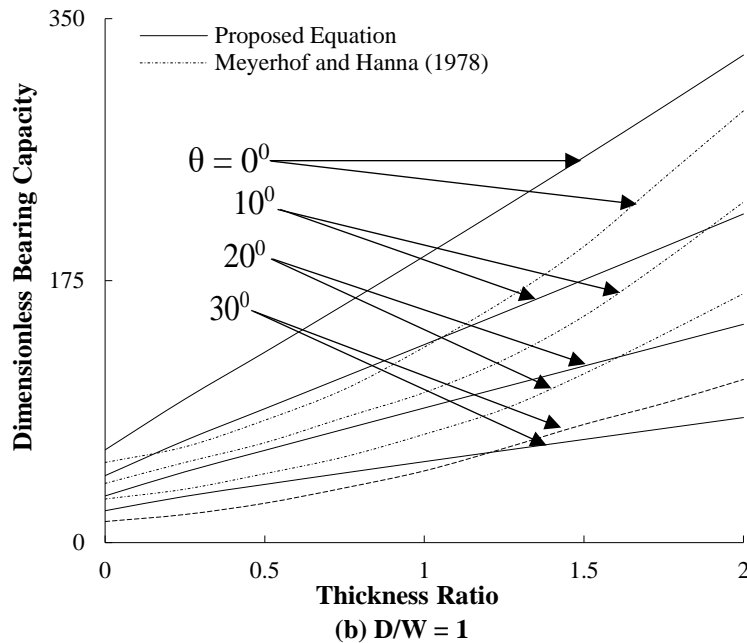


Fig. 8. Comparison of the rectangular footing at $L/W=1$ with circular footing

The results obtained from the proposed Eq. (19) were higher than the results obtained from Meyerhof and Hanna (1978) for higher thickness ratios (> 0.25). The average deviation in the results obtained from the proposed Eq. (19) was about 15.61% in comparison to the results reported by Meyerhof and Hanna (1978). Further, from Figure 8b, at $D/W = 1$, the results obtained from the proposed Eq. (19) were more conservative in comparison to the results obtained at $D/W = 0$ when compared with the results of Meyerhof and Hanna (1978). Further, study of Figure 8b reveals that the average deviation in the dimensionless bearing capacity was about 10.71% in case of embedded footing. All discrepancy may be due to the difference in the actual shape of the footings used in the comparison at the same shape factor, as well as the fact that the load spread angle used by Meyerhof and Hanna (1978) was assumed to be equal to the angle of load inclination.

5. Conclusions

In the present study, the bearing capacity equation for rectangular footing subjected to inclined load and resting on the layered sand (dense sand overlying loose sand) was

derived using a well-known limit equilibrium methodology along with load spread mechanism. The results obtained from this study bring forth the following conclusions:

- The highest and the lowest increase in the bearing capacity was observed at a friction angle combination of 46° - 36° and 41° - 31° respectively, at varying thickness ratio.
- The bearing capacity obtained from the proposed equation was approximately 4.97 and 10.5 times of its initial value at an embedment ratio 1 and 2, respectively.
- For $\phi_1 = 46^{\circ}$ and $\phi_2 = 36^{\circ}$ and at a thickness ratio of 2.00, the bearing capacity at a load inclination of 5° , 15° and 30° decreased about 20.55%, 54.58% and 87.90% of its initial value.
- The decrease in the bearing capacity obtained from the proposed equation was 99.89%, 66.04% and 61.5% with the increase in the load inclination from 0° to 30° for an embedment ratio 0, 1 and 2, respectively.
- In comparison to the proposed equation estimates, the average deviation was 14.56%, 18.71% and 23.56% for embedment ratio 0, 1 and 2, respectively with respect to finite element results.

- The results obtained from the derived bearing capacity equation was found to be comparable with those reported in literature with an average deviation of about 10.71% at different embedment ratio.

6. List of Symbols

φ_1, φ_2	Soil friction angle for upper dense sand and lower loose sand soil, in degree
γ_1, γ_2	Unit weight of the upper dense sand soil and lower loose sand soil, kN/m ³
$\alpha_1, \alpha_2,$ and $\alpha_3,$ α_4	Load dispersion angle across width and length of the footing in general form, degree
E_1, E_2	Elastic moduli for upper dense sand and lower loose sand layer
ν_1, ν_2	Poissons ratio for upper layer and lower layer
W	Width of the footing
L	Length of the footing
Δz	Small strip thickness
θ	Concentric load inclination angle with respect to vertical acting on the rectangular footing, in degree
σ	Stress applied on the footing, kN/m ²
σ_v	Vertical component of the applied stress, kN/m ²
q_u	Concentrated inclined load acting, kN
H	Thickness of the upper dense sand layer
D	Depth of the embedded footing from ground surface
P_p	Total passive earth pressure acting normal to the failure plane
P_{pv}	Vertical component of passive earth pressure
ΔP_p	Small passive earth pressure acting on small strip soil
K_p	Passive earth pressure coefficient
q_{uv}	Ultimate load bearing capacity of the rectangular footing in the layered sand (vertical component)
q_{Lv}	Ultimate bearing capacity of lower loose sand (vertical component)
q_u	Ultimate bearing capacity of upper dense sand (vertical component)
i_q, i_γ	Inclination factors
S_γ, S_q	Shape factors
N_q, N_γ	Bearing capacity
d_q, d_γ	Depth factors
C	Constant of integration
$\left(\frac{q_{uv}}{\gamma_1 W}\right)$	Dimensionless ultimate bearing capacity of the footing
δ	Mobilised shearing resistance angle at failure, degree

Z	Distance where small strip of soil lies below rectangular footing
H/W	Thickness ratio
D/W	Embedment ratio
φ_2/φ_1	Soil friction ratio

7. Acknowledgment

The authors would like to express special thanks to Central Building Research Institute (CSIR-CBRI) Roorkee for providing the opportunity to utilize the ABAQUS software for this work.

8. References

- Al-Ameri, A.F.I., Hussein, S.A. and Mekkiyah, H. (2020). "Estimate the bearing capacity of full-scale model shallow foundations on layered-soil using PLAXIS", *Solid State Technology*, 63(1), 1775-1787, <http://solidstatetechnology.us/index.php/JSST/article/view/568>.
- Benmoussa, S., Benmebarek, S. and Benmebarek, N. (2021). "Bearing capacity factor of circular footings on two-layered clay soils", *Civil Engineering Journal*, 7(5), 775-785, <https://doi.org/10.28991/cej-2021-03091689>.
- Biswas, A. and Krishna, A.M. (2019). "Behaviour of circular footing resting on layered foundation: sand overlying clay of varying strengths", *International Journal of Geotechnical Engineering*, 13(1), 9-24, <https://doi.org/10.1080/19386362.2017.131424>.
- Bowles, J.E. (1977). *Foundation analysis and design*, McGraw-Hill, New York.
- Caquot, A., and Kerisel, L. (1949). *Traite de mecanique des sols*, Gauthier-Villars, Paris, France.
- Chwała M. and Puła W. (2020). "Evaluation of shallow foundation bearing capacity in the case of a two-layered soil and spatial variability in soil strength parameters", *Plos One*, 15(4), e0231992, <https://doi.org/10.1371/journal.pone.0231992>.
- Das, P. and Khatri V. (2021). "Bearing capacity estimation of shallow foundations on layered sand strata using finite elements analysis", *Lecture Notes in Civil Engineering book series*, 137, 401-412, https://doi.org/10.1007/978-981-33-6466-0_37.
- Das, P.P., Khatri, V.N. and Dutta, R.K. (2021). "Bearing capacity of ring footing on a weak sand layer overlying a dense sand deposit", *Geomechanics and Geoenvironment*, 16(4), 249-262, <https://doi.org/10.1080/17486025.2019.1664775>.

- Das, P.P., Khatri, V.N. and Kumar, J. (2022). "Bearing capacity of strip and circular footing on layered sand with geogrid at the interface", *Arabian Journal of Geosciences*, 15(1), 361, <https://doi.org/10.1007/s12517-022-09614-1>.
- Dawarci, B., Ornek, M. and Turedi, Y. (2014). "Analysis of multi-edge footings rested on loose and dense sand", *Periodica Politechnica Civil Engineering*, 58(4), 355-370, <https://doi.org/10.3311/PPci.2101>.
- El-Kasabi, E.A.A. (1991). "Estimation of guide values for the modulus of elasticity of soil", *Bulletin of Faculty of Engineering HRBC Journal*, 19(1), 1-7.
- Eshkevari, S.S., Abbo, A.J. and Kouretzis, G.P. (2018). "Bearing capacity of strip footings on sand over clay", *Canadian Geotechnical Journal*, 56(5), 1-33, <https://doi.org/10.1139/cgj-2017-0489>.
- Eshkevari, S.S., Abbo, A.J. and Kouretzis, G. (2019). "Bearing capacity of strip footings on layered sands", *Computers and Geotechnics*, 114(1 October), 103101, <https://doi.org/10.1016/j.compgeo.2019.103101>.
- Farah, C.A. (2004). "Ultimate bearing capacity of shallow foundations on layered soils", MSc Thesis, Civil and Environmental Engineering, Concordia University, Quebec.
- Gupta, S. and Mital, A. (2021). "A comparative study of bearing capacity of shallow footing under different loading conditions", *Geomechanics and Geoengineering*, 17(4), 1338-1349, <https://doi.org/10.1080/17486025.2021.1940310>.
- Hajitaheriha, M.M., Jafari, F., Hassanlourad, M. and Motlagh, A.H. (2021). "Investigating the reliability of negative skin friction on composite piles", *Civil Engineering Infrastructures Journal*, 54(1), 23-42, <https://doi.org/10.22059/CEIJ.2020.287489.1607>.
- Hanna, A.M. (1981). "Foundations on strong sand overlying weak sand", *Journal of the Geotechnical Engineering*, 107(7), 915-927.
- Hanna, A.M. (1982). "Bearing capacity of foundations on a weak sand layer overlying a strong deposit", *Canadian Geotechnical Journal*, 19(3), 392-396, <https://ascelibrary.org/doi/10.1061/AJGEB6.0001169>.
- Hanna, A.M. (1987). "Finite element analysis of footings on layered soils", *Mathematical Modelling*, 9(11), 813-819, <https://doi.org/10.1139/t82-043>.
- Ibrahim, K.M.H.I. (2016). "Bearing capacity of circular footing resting on granular soil overlying soft clay", *Housing and Building National Research Center Journal*, 1(1), 71-77, <https://doi.org/10.1016/j.hbrcj.2014.07.004>.
- Ibrahim, M.M., and Al-Obaydi, M.A. (2021). "Numerical analysis of a rectangular footing resting on two inclined layers of soil", *IOP Conference Series: Earth and Environmental Science*, (Vol. 856, No. 1, p. 012039), IOP Publishing, <https://doi.org/10.1088/1755-1315/856/1/012039>.
- IS 6403 (1981). *Code of practice for determination of breaking capacity of shallow foundations*, Bureau of Indian Standard, New Delhi, India.
- Johnson, K., Christensen, M., Sivakugan, N. and Karunasena, W. (2015). "Simulating the response of shallow foundations using finite element modelling", *Proceedings of the MODSIM 2003 International Congress on Modelling and Simulation*, Townsville, QLD, Australia (pp. 14-17), https://www.mssanz.org.au/MODSIM03/Volume_04/C15/03_Johnson_Simulating.pdf.
- Kenny, M.J. and Andrawes, K.Z. (1997). "The bearing capacity of footings on a sand layer overlying soft clay", *Geotechnique*, 47(2), 339-345, <https://doi.org/10.1680/geot.1997.47.2.339>.
- Khatri, V.N., Debbarma, S.P., Dutta, R.K. and Mohanty, B. (2017b). "Pressure-settlement behaviour of square and rectangular skirted footings resting on sand", *Geomechanics and Engineering*, 12(4), 689-705, <https://doi.org/10.12989/gae.2017.12.4.689>.
- Khatri, V.N., Kumar, J. and Akhtar, S. (2017a). "Bearing capacity of foundations with inclusion of dense sand layer over loose sand strata", *International Journal of Geomechanics*, 17(10), 06017018, [https://doi.org/10.1061/\(ASCE\)GM.1943-5622.0000980](https://doi.org/10.1061/(ASCE)GM.1943-5622.0000980).
- Kumar, A., Ohri, M.L. and Bansal R.K. (2007). "Bearing capacity tests of strip footings on reinforced layered soil", *Geotechnical and Geological Engineering*, 25(2), 139-150, <https://doi.org/10.1007/s10706-006-0011-6>.
- Mandeel, S.A.H., Mekkiyahb H.M. and Al-Americ, A.F.I. (2021). "Bearing Capacity of square footing resting on layered soil", *Al-Qadisiyah Journal for Engineering Sciences*, 13, 306-313, <https://doi.org/10.30772/qjes.v13i.700>.
- Massihv, D.Y.A., Hachem, E.E. and Soubra, A.H. (2005). "Bearing capacity of eccentrically and/or obliquely loaded strip footing over two-layer foundation soil by a kinematical approach", *VIII International Conference on Computational Plasticity (COMPLAS VIII)*, Barcelona.
- Merifield, R.S., Sloan, S.W. and Yu, H.S. (1999). "Rigorous plasticity solutions for the bearing capacity of two-layered clays", *Géotechnique*, 49(4), 471-490, <https://doi.org/10.1680/geot.1999.49.4.471>.
- Meyerhof, G.G. (1974). "Ultimate bearing capacity of footings on sand layer overlying clay",

- Canadian Geotechnical Journal*, 11(2), 223-229, <https://doi.org/10.1139/t74-018>.
- Meyerhof, G.G. and Hanna, A.M. (1978). "Ultimate bearing capacity of foundations on layered soils under inclined load", *Canadian Geotechnical Journal*, 15(4), 565-572, <https://doi.org/10.1139/t78-060>.
- Michalowski, R.L. and Shi, L. (1995). "Bearing capacity of footings over two-layer foundation soil", *Journal of the Geotechnical Engineering*, 121(5), 421-428, <https://ascelibrary.org/doi/10.1061/%28ASCE%290733-9410%281995%29121%3A5%28421%29>.
- Misir, G. and Laman, M. (2017). "A modern approach to estimate the bearing capacity of layered soil", *Periodica Polytechnica Civil Engineering*, 61(3), 434-446, <https://doi.org/10.3311/PPci.9578>.
- Mosadegh, A. and Nikraz, H. (2015). "Bearing capacity evaluation of footing on a layered-soil using ABAQUS", *Journal of Earth Science and Climatic Change*, 6(3), 264, <http://dx.doi.org/10.4172/2157-7617.1000264>.
- Nujid, M.M., Idrus, J., Bawadi, N.F. and Firoozi, A. A. (2021). "Evaluating the effect of embedment depth on collapse failure analysis of strip foundation", *Civil Engineering and Architecture*, 9(5A), 1-9, <https://doi.org/10.13189/cea.2021.091301>.
- Oda, M. and Win, M. (1990). "Ultimate bearing-capacity tests on sand with clay layer", *Journal of the Geotechnical Engineering*, 116(12), 1902-1906, [https://doi.org/10.1061/\(asce\)0733-9410\(1990\)116:12\(1902\)](https://doi.org/10.1061/(asce)0733-9410(1990)116:12(1902)).
- Okamura, M., Takemura, J. and Kimura, T. (1998). "Bearing capacity predictions of sand overlying clay based on limit equilibrium methods", *Soils and Foundations*, 38(1), 181-194, <https://doi.org/10.3208/sandf.38.181>.
- Panwar, V. and Dutta, R.K. (2021). "Bearing capacity of rectangular footing on layered sand under inclined loading", *Journal of Achievements in Materials and Manufacturing Engineering*, 108(2), 49-62, <https://doi.org/10.5604/01.3001.0015.5064>.
- Rao, P., Liu, Y. and Cuia, J. (2015). "Bearing capacity of strip footings on two-layered clay under combined loading", *Computers and Geotechnics*, 69, 210-218, <https://doi.org/10.1016/j.compgeo.2015.05.018>.
- Reddy, V.S.K. and Kumar D.T.K. (2018), "Behaviour of foundation in layered soils", *International Journal of Science and Research*, 7(1), 1075-1078, <https://doi.org/10.21275/ART20179556>.
- Saha, A., Patra, S., Das, A. and Bera, A.K. (2018). "Bearing capacity of footing on sand overlay by soft soil using Abaqus: A numerical based study", *Geotechnics for Infrastructure Development*, Indian Geotechnical Society, Kolkata Chapter.
- Shiau, J.S., Lyamin, A.V. and Sloan, S.W. (2003). "Bearing capacity of a sand layer on clay by finite element limit analysis", *Canadian Geotechnical Journal*, 40(5), 900-915, <https://doi.org/10.1139/t03-042>.
- Shoaei, M.D., Alkarni, A., Noorzaeei, J., Jaafar, M.S. and Huat, B.B.K. (2012). "Review of available approaches for ultimate bearing capacity of two-layered soils", *Journal of Civil Engineering and Management*, 18(4), 469-482, <https://doi.org/10.3846/13923730.2012.699930>.
- Singh, S.P. and Roy, A.K. (2021). "Numerical study of the behaviour of a circular footing on a layered granular soil under vertical and inclined loading", *Civil and Environmental Engineering Reports*, 1(31), 29-43, <https://doi.org/10.2478/ceer-2021-0002>.
- Szypcio, Z. and Dołżyk, K. (2006). "The bearing capacity of layered subsoil", *Studia Geotechnica et Mechanica*, XXVIII(1), 45-60.
- Ullah, S.N., Hossain, M.S., Hu, Y. and Fourie, A. (2020). "Numerical modelling of rectangular footing on a sand embankment over mine tailings", In: Wang, C., Ho, J., Kitipornchai, S. (eds.), *ACMSM25, Lecture Notes in Civil Engineering*, Springer, Singapore; 37, 1027-1036, https://doi.org/10.1007/978-981-13-7603-0_97.
- Zheng, G., Zhao, J., Zhou, H. and Zhang, T. (2019). "Ultimate bearing capacity of strip footings on sand overlying clay under inclined loading", *Computers and Geotechnics*, 106(1 February), 266-273, <https://doi.org/10.1016/j.compgeo.2018.11.003>.



This article is an open-access article distributed under the terms and conditions of the Creative Commons Attribution (CC-BY) license.